Human activated protein C attenuates both hepatic and renal injury caused by hepatic ischemia and reperfusion injury in mice

Sang Won Park[1], Sean W.C. Chen[1], Mihwa Kim[1], Vivette D. D'Agati[2] and H. Thomas Lee[1]

[1]*Department of Anesthesiology, College of Physicians and Surgeons of Columbia University, New York, New York, USA and* [2]*Department of Pathology, College of Physicians and Surgeons of Columbia University, New York, New York, USA*

Hepatic ischemia and reperfusion (IR) injury is a major clinical problem often leading to acute kidney injury characterized by early endothelial cell apoptosis, subsequent neutrophil infiltration, proximal tubule necrosis/inflammation, impaired vascular permeability, and disintegration of the proximal tubule filamentous actin cytoskeleton. Activated protein C is a major physiological anticoagulant with anti-inflammatory and anti-apoptotic activities in endothelial cells. Here we tested if activated protein C would attenuate hepatic and renal injury caused by hepatic ischemia and reperfusion. Both liver and kidney injury were significantly reduced when activated protein C was given immediately before and 2 h after liver reperfusion, in that there was reduced renal endothelial and hepatocyte apoptosis, as well as reduced hepatic and renal tubular necrosis. Further, the administration of activated protein C also reduced the expression of several pro-inflammatory genes, liver and kidney filamentous-actin degradation, and neutrophil infiltration, and resulted in better preservation of vascular permeability of both the liver and kidney than is normally seen after liver ischemia and reperfusion. These protective effects of activated protein C were due to protease-activated receptor-1 modulation since administration of a selective receptor antagonist dose-dependently inhibited its ameliorative effects in both organs after liver ischemia and reperfusion. Our results suggest the powerful multi-organ protective effects of activated protein C may improve outcome in those patients at significant risk of developing acute kidney injury following liver ischemia and reperfusion during transplantation.

Kidney International (2009) **76,** 739–750; doi:10.1038/ki.2009.255; published online 22 July 2009

KEYWORDS: apoptosis; inflammation; kidney; liver; necrosis; neutrophil

Correspondence: *H. Thomas Lee, Department of Anesthesiology, Anesthesiology Research Laboratories, Columbia University, P&S Box 46 (PH-5), 630 West 168th Street, New York, New York 10032-3784, USA. E-mail: tl128@columbia.edu*

Received 4 March 2009; revised 30 April 2009; accepted 19 May 2009; published online 22 July 2009

Hepatic ischemia and reperfusion (IR) is a common problem encountered in many clinical conditions including liver transplantation, major hepatic resection, and prolonged portal vein occlusion.[1,2] The pathophysiology of hepatic IR injury is complex and involves complex orchestration of necrosis, apoptosis, and inflammation of hepatic (hepatocytes, Kupffer cells) and extra-hepatic (leukocytes, circulating cytokines) components. Hepatic IR frequently leads to remote organ injury including the kidney, lung, and heart.[3,4] In particular, acute kidney injury (AKI) after major liver IR is extremely common (40–85% incidence) and the development of AKI after liver injury implies high mortality and morbidity during the perioperative period. We recently developed a murine model of liver IR-induced AKI characterized by early renal endothelial apoptosis and dysfunction, proximal tubule inflammation, and necrosis.[5] Liver IR-induced AKI also produced severe impairment in vascular permeability of the liver and the kidney together with filamentous (F)-actin degradation.[5] Therefore, AKI developed because liver IR is a disease of early endothelial apoptosis and dysfunction, renal inflammation with subsequent F-actin degradation, and tubular necrosis.

Activated protein C (APC) is a serine protease with powerful anticoagulant activities in endothelial cells.[6] In addition to its effects on coagulation, APC also exerts anti-inflammatory, antiapoptotic and cytoprotective effects.[7] Moreover, APC promotes microvascular integrity, provides powerful endothelial barrier protection, and disrupts the amplification of coagulation defects secondary to an uncontrolled inflammatory response after IR injury or severe sepsis.[8] Soluble thrombomodulin, an important co-factor of thrombin-mediated cleavage and activation of protein C, provided powerful protection against hypoperfusion-induced AKI in rats when given before or after ischemic injury.[9] Based on these protective effects, APC has been considered as a potent prophylactic and/or therapeutic agent to attenuate microvascular injury, inflammatory response, and septic shock.[10] Recently, there are reports showing that APC prevents post-ischemic damage in the brain,[11] heart,[12] and intestine[13] after IR. All of the protective effects of APC (endothelial protection, reduction in apoptosis,

inflammation, and preservation of microvascular permeability) would negate the pathological changes observed in liver IR injury and subsequent AKI.

Therefore, in this study, we examined whether APC treatment could protect against both hepatic and renal injury induced by hepatic IR. We show that APC treatment improved renal and hepatic function after liver IR. We also demonstrate that mice treated with APC benefited significantly with a reduced inflammatory response, better preservation of microvascular permeability, less disruption of the F-actin cytoskeleton, and reduced apoptotic changes of the liver and kidney after severe liver IR injury. We also demonstrate that the protective effects of APC is due to protease-activated receptor-1 (PAR-1) modulation as a selective PAR-1 receptor antagonist (SCH 79797) dose-dependently inhibited APC's protective effects against liver and kidney injury after liver IR.

RESULTS

APC treatment protects against hepatic and renal injury after liver IR

The plasma level of alanine aminotransferase (ALT) and creatinine (Cr) in the sham-operated mice was 62 ± 8 U/l ($N=6$) and 0. 41 ± 0.04 mg per 100 ml ($N=7$), respectively. APC treatment produced dose (40–250 μg/kg i.v. before reperfusion and 80–500 μg/kg s.c. 2 h after reperfusion) dependent protection against liver as well as renal injury 24 h after liver IR (Figure 1). In the saline-IR group, the plasma level of ALT and Cr increased at 5 (ALT = 20097 ± 1434 U/l, $N=8$, $P<0.01$ vs Sham, and Cr = 0.60 ± 0.09 mg per 100 ml, $N=8$) and 24 h (ALT = 15211 ± 1190 U/l, $N=8$, $P<0.01$ vs Sham, and Cr = 1.11 ± 0.10 mg per 100 ml, $N=8$, $P<0.01$ vs Sham) after reperfusion. The increases in ALT were significantly suppressed by APC treatment (250 μg/kg i.v. before reperfusion and 500 μg/kg s.c. 2 h after reperfusion) at 5 h (ALT = 12118 ± 1369 U/l, $N=6$, $P<0.01$) and 24 h (ALT = 6276 ± 1107 U/l, $N=8$, $P<0.001$) after reperfusion. The increases in Cr were significantly suppressed by APC treatment (250 μg/kg i.v. before reperfusion and 500 μg/kg s.c. 2 h after reperfusion) at 24 (Cr = 0.29 ± 0.06 mg per 100 ml, $N=6$, $P<0.001$) but not at 5 h (Cr = 0.49 ± 0.09 mg per 100 ml, $N=6$, NS) after reperfusion. The urinary ALT was nearly undetectable in sham-operated mice (ALT = 0.6 ± 0.3 U/l, $N=7$) and did not significantly increase in mice subjected to liver IR (ALT = 14.8 ± 11 U/l, $N=8$, $P=0.25$). The survival rates for saline- (70%, $N=20$) or APC-treated (90%, $N=10$) mice were not statistically different at 24 h after liver IR (χ^2 test).

We also tested whether the blockade of protease-activated receptor-1 (PAR-1) would prevent the renal and hepatic protective effects of APC after liver IR. We used SCH 79797 (N3-cyclopropyl-7-{[4-(1-methylethyl)phenyl]methyl}-7H-pyrrolo[3,2-f]quinazoline-1,3 diamine, Tocris Bioscience, Ellisville, Missouri, USA) to block PAR-1 and then administered APC in mice subjected to liver IR. SCH 79797 in a dose-dependent manner (0.02–0.5 mg/kg) prevented the hepatic and renal protective effects of APC treatment (250 μg/kg i.v. before reperfusion and 500 μg/kg s.c. 2 h after reperfusion) at 5 h (not shown) and at 24 h after liver IR in mice (Figure 1c and d). We also noted that an intermediate dose of this PAR-1 antagonist (0.1 mg/kg SCH 79797) produced moderate hepatic (but not renal) protection after liver IR (Figure 1c).

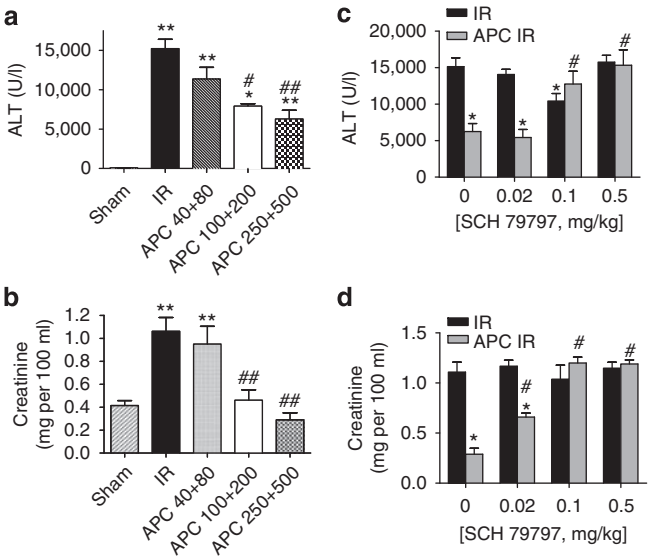

Figure 1 | APC protects liver and kidney against hepatic IRI. (**a** and **b**). Dose-dependent protective effects of APC against hepatic (**a**, ALT) and renal (**b**, creatinine) injury in C57BL/6 mice subjected to sham operation (sham), saline treatment, and liver ischemia and reperfusion (IR) or APC treatment during and after liver IR (APC + IR). Three doses of APC were given to mice: 40 μg/kg i.v. before reperfusion and 80 μg/kg s.c. 2 h after reperfusion (40 + 80), 100 μg/kg i.v. before reperfusion and 200 μg/kg s.c. 2 h after reperfusion (100 + 200), or 250 μg/kg i.v. before reperfusion and 500 μg/kg s.c. 2 h after reperfusion (250 + 500). $^{**}P<0.01$ vs sham group. $^{\#}P<0.05$ and $^{\#\#}P<0.01$ vs IR group. (**c** and **d**). SCH 79797 (N3-Cyclopropyl-7-[[4-(1-methylethyl)phenyl]methyl]-7H-pyrrolo[3,2-f]quinazoline-1,3-diamine-dihydrochloride) in a dose-dependent manner (0.02–0.5 mg/kg) prevented the hepatic (**c**) and renal protective effects (**d**) of APC treatment (250 μg/kg i.v. before reperfusion and 500 μg/kg s.c. 2 h after reperfusion) at 5 h (not shown) and at 24 h after liver IR in mice. $^{*}P<0.01$ vs vehicle-treated IR group. $^{\#}P<0.05$ vs APC IR group. Data are presented as mean ± s.e.m.

APC treatment reduces hepatic necrosis after IR

Representative histological slides (magnification, × 40) from liver tissues from saline-treated and APC-treated mice subjected to 60 min ischemia and 24 h reperfusion or to sham operation are shown in Figure 2. Sixty minutes of partial hepatic IR produced large necrotic areas of livers after reperfusion (Figure 2a). Correlating with significantly improved function, reduced necrosis was observed in mice treated with APC and subjected to hepatic IR (Figure 2a). The average percent necrotic areas for saline-treated mice were $61 \pm 6\%$ ($N=7$) and APC-treatment reduced this percent necrosis to $38 \pm 8\%$ ($N=7$, $P<0.03$). We failed to detect necrosis in liver sections from sham-operated mice. Livers were also analyzed for the degree of hepatocellular

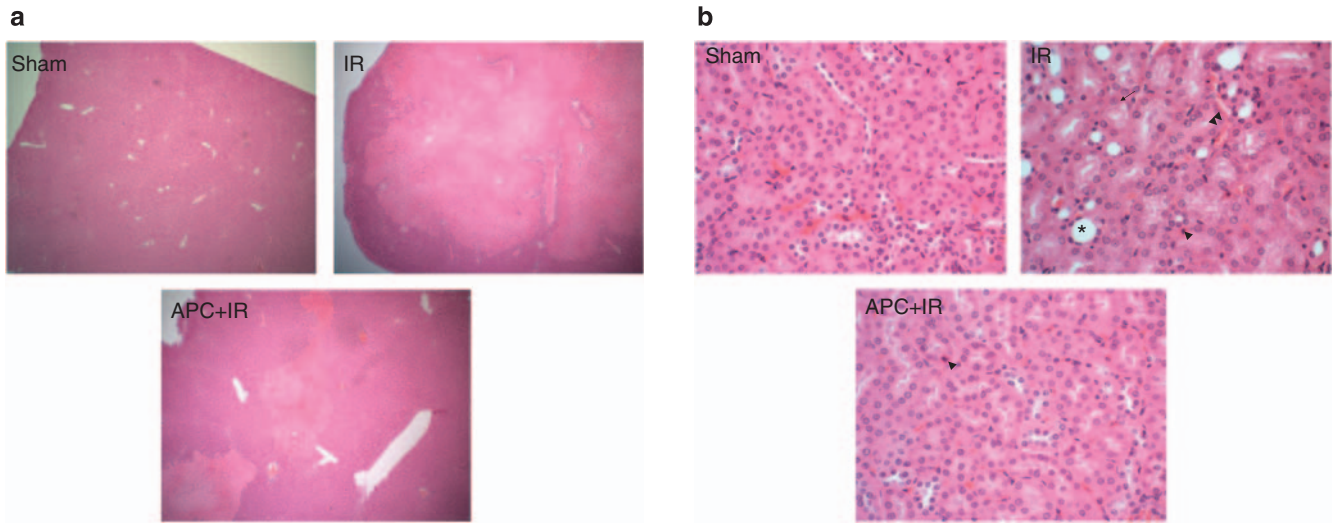

Figure 2 | APC improves histology after liver IRI in the liver and kidney. Representative photomicrographs of hematoxylin and eosin staining of the liver (**a**, ×40) and kidney (**b**, ×200) sections. C57BL/6 mice were subjected to sham operation (sham), saline treatment, and liver ischemia and reperfusion (IR) or APC treatment during and after liver IR (APC + IR), and the liver and kidney sections were obtained 24 h after reperfusion. *A representative dilated tubule from simplification, arrow indicates cytoplasmic vacuolization, arrowhead indicates hypereosinophilic tubule cell death, and double arrowhead indicates peritubular vascular stasis. Photographs are representative of six independent experiments.

damage using Suzuki's criteria.[14] The ischemic lobes in the control group showed severe hepatocyte necrosis and sinusoidal congestion (Suzuki score = 10.7 ± 0.6, $N = 6$). Mice treated with APC revealed significantly less necrosis/sinusoidal congestion and better preservation of lobular architecture (Suzuki score = 7.8 ± 0.7, $N = 6$, $P < 0.01$).

APC treatment reduces renal cortical vacuolization, proximal tubular simplification, and hypereosinophilia after liver IR

When we examined the kidneys from the mice injected with saline vehicle and subjected to liver IR, we observed multifocal acute tubular injury including S3 segment proximal tubule necrosis, cortical tubular simplification, cytoplasmic vacuolization, and dilated lumina as well as focal granular bile/heme casts (Figure 2b). Representative H&E slides from kidneys from saline-treated and APC-treated mice subjected to 60 min ischemia and 24 h reperfusion or to sham operation are shown in Figure 2b (magnification, × 200). Correlating with significantly improved renal function, mice treated with APC showed less renal tubular hypereosinophilia and cortical vacuolization (Figure 2b).

APC treatment reduces hepatic and renal neutrophil infiltration 24 h after liver IR

Figure 3 shows representative images of neutrophil immunohistochemitry of liver (A, magnification × 100) and kidney (B, magnification × 400) sections from mice subjected to sham operation or to 60 min of liver ischemia and 24 h reperfusion. In sham-operated mice, we were unable to detect any neutrophils in the liver or kidney. Sixty minutes of hepatic ischemia and 24 h reperfusion resulted in recruitment of neutrophils into the liver (Figure 3a). Neutrophil infiltration coincided with areas of liver necrosis. Subsequently, although mice treated with APC and subjected to liver IR had reduced areas of liver necrosis, the number of neutrophils present in the necrotic areas visualized (19.8 ± 6.2 neutrophils/field, × 200 magnification, $N = 6$) was similar to the animals subjected to liver IR after vehicle (saline) injection (24.2 ± 1.7 neutrophils/field, × 200 magnification, $N = 6$, Figure 3a).

Sixty minutes of hepatic ischemia also resulted in recruitment of neutrophils into the kidney (Figure 3b). Neutrophil infiltration 24 h after hepatic ischemia was significantly less in APC-treated mice compared with the saline-treated mice subjected to liver IR. Twenty-four hours after liver IR, we detected 9.3 ± 3.4 neutrophils/field (× 200 magnification, $N = 5$) in saline-treated mice subjected to liver IR. APC-treated mice had significantly reduced neutrophil infiltration 24 h after liver IR (1.3 ± 0.9 neutrophils/field, × 200 magnification, $N = 5$, $P < 0.05$).

APC-treatment decreases hepatic and renal vascular permeability after liver IR

We measured liver vascular permeability after liver IR with Evans blue dye (EBD) injection. EBD binds to plasma proteins and its appearance in extravascular tissues reflects an increase in vascular permeability. Analysis of EBD extravasations in saline- and APC-treated mice subjected to sham-operation and liver IR are shown in Figure 4. Liver IR increased the EBD content in the liver for both groups, however, the increase in EBD content was significantly higher for the saline-treated mice (376.5 ± 37.4 μg EBD/g dry liver, $N = 6$) compared with the APC-treated mice (167.5 ± 22.8 μg EBD/g dry liver, $N = 6$, $P < 0.001$). Liver IR also increased the EBD content in the kidney for both groups, however, the increase in EBD content was significantly higher for the

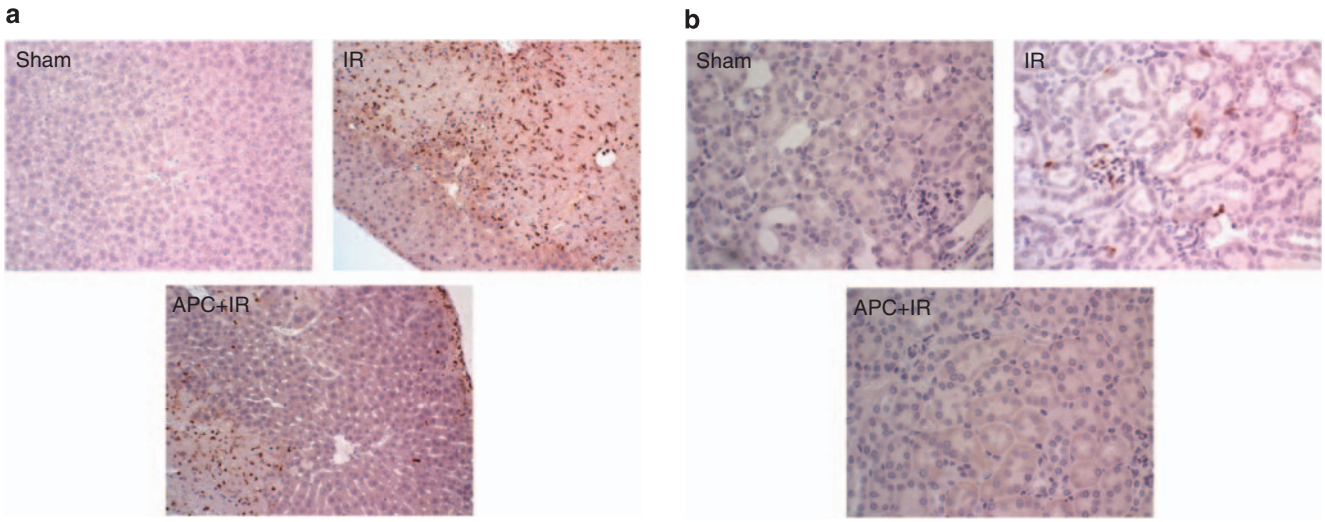

Figure 3 | APC reduces neutrophil infiltration after liver IRI in the liver and kidney. Representative of photomicrographs of immunohistochemistry for neutrophils in liver (**a**, ×200) and kidney (**b**, ×400) sections. C57BL/6 mice were subjected to sham operation (sham), saline treatment, and liver ischemia and reperfusion (IR) or APC treatment during and after liver IR (APC + IR) and the liver and kidney sections were obtained 24 h after reperfusion. Photographs are representative of six independent experiments.

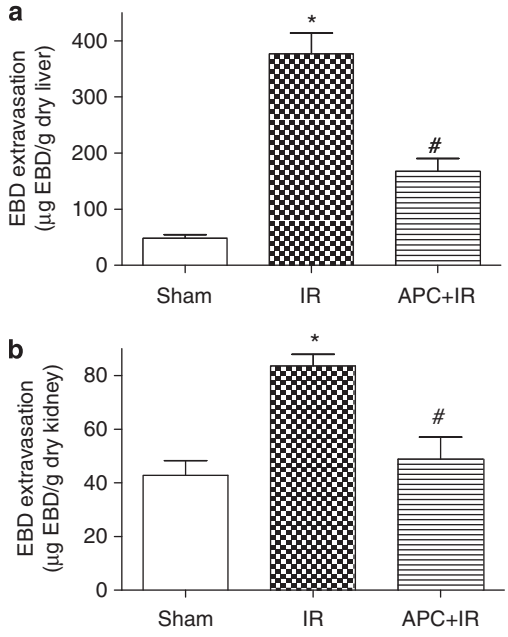

Figure 4 | APC improves vascular permeability after liver IRI in the liver and kidney. Evans blue dye (EBD) extravasations as indices of vascular permeability of liver (**a**) and kidney (**b**) tissues in C57BL/6 mice subjected to sham operation (sham), saline treatment, and liver ischemia and reperfusion (IR) or APC treatment during and after liver IR (APC + IR). The liver and kidney tissues were obtained 24 h after reperfusion. Data are presented as means ± s.e.m. *$P<0.001$ vs sham group. #$P<0.001$ vs IR group.

saline-treated mice (83.5 ± 4.3 μg EBD/g dry kidney, $N=6$) compared with the APC-treated mice (48.8 ± 8.2 μg EBD/g dry kidney, $N=6$, $P<0.001$).

APC treatment reduces plasma TNF-α after liver IR

In sham-operated animals, the plasma TNF-α level was not detectable. In contrast, the plasma TNF-α level increased markedly to 852.3 ± 80.8 pg/ml ($N=4$) 24 h after liver IR. However, this increase was attenuated by APC treatment (23.5 ± 23.5 pg/ml, $N=4$, $P<0.001$, Figure 5).

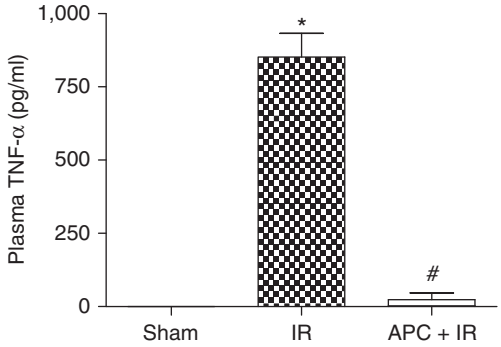

Figure 5 | Plasma TNF-α levels in C57BL/6 mice subjected to sham operation (sham), saline treatment, and liver ischemia and reperfusion (IR) or APC treatment during and after liver IR (APC + IR). The blood samples were collected 24 h after reperfusion. Data are presented as mean ± s.e.m. *$P<0.001$ vs sham group. #$P<0.001$ vs IR group.

APC treatment reduces TNF-α mRNA in the liver and MCP-1 and MIP-2 mRNA in the kidney after liver IR

We measured the expression of pro-inflammatory cytokine mRNAs in the liver and the kidney at 5 h and 24 h after liver IR with semi-quantitative RT-PCR. Hepatic IR was associated with significantly increased pro-inflammatory mRNA expression at 5 h (ICAM-1, TNF-α, KC, MCP-1, and MIP-2) in the liver (Figure 6) as well as in the kidney (Figure 7) from saline-treated mice compared with the sham-operated mice. These increases in pro-inflammatory mRNA expression were also observed at 24 h after reperfusion (data not shown). However, APC-treated mice showed significantly reduced

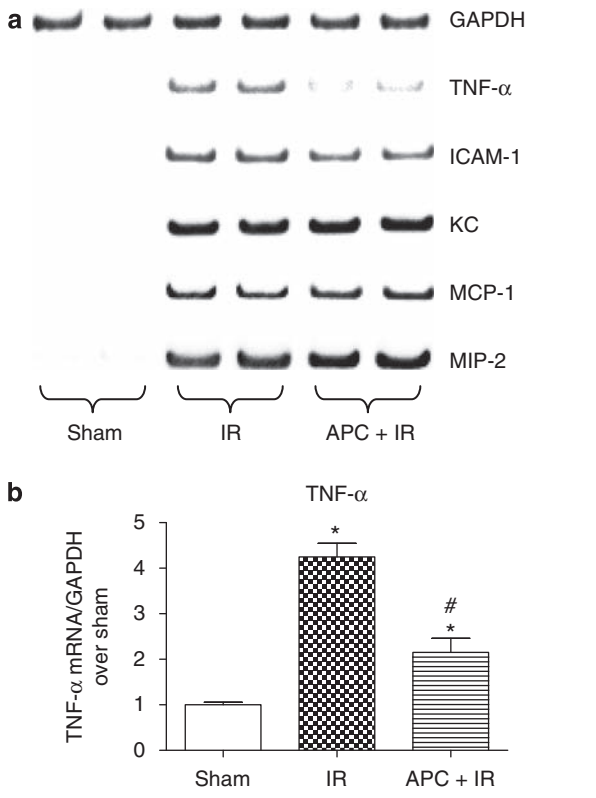

Figure 6 | Effect of APC on pro-inflammatory gene expression in the liver after hepatic IR. (**a**) Representative gel images of RT-PCR results for GAPDH, TNF-α, ICAM-1, KC, MCP-1, and MIP-2 mRNAs of liver tissue. C57BL/6 mice were subjected to sham operation (sham), saline treatment, and liver ischemia and reperfusion (IR) or APC treatment during and after liver IR (APC + IR). The liver tissues were obtained 5 h after reperfusion. (**b**) Densitometric quantification of relative TNF-α band intensities normalized to GAPDH from RT-PCRs. Data are presented as means ± s.e.m. $^{*}P<0.05$ vs sham group. $^{\#}P<0.05$ vs IR group.

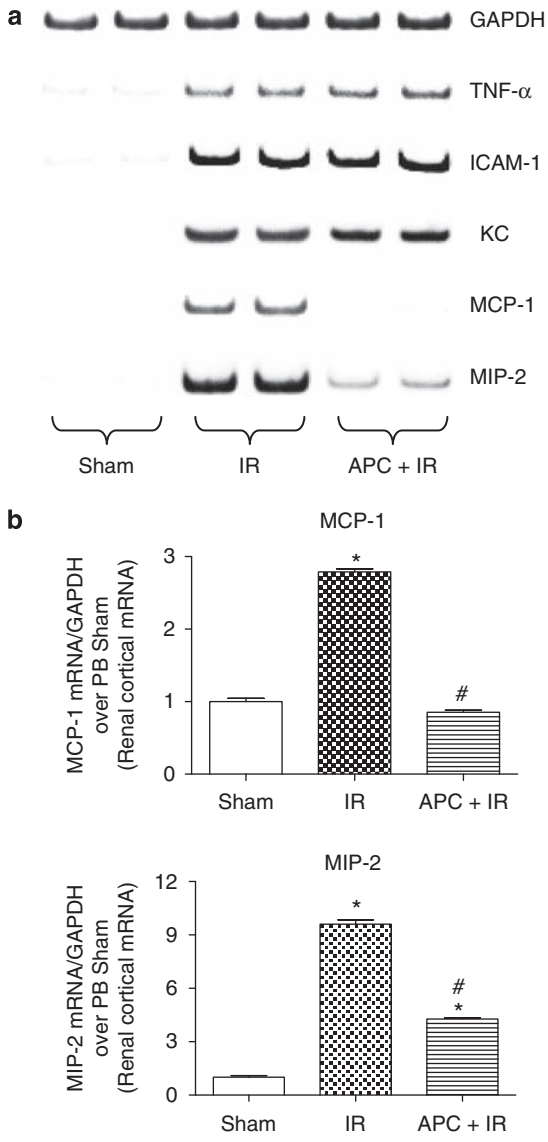

Figure 7 | Effect of APC on pro-inflammatory gene expression in the kidney after hepatic IR. (**a**) Representative gel images of semi-quantitative RT-PCR results for GAPDH, TNF-α, ICAM-1, KC, MCP-1, and MIP-2 mRNAs of kidney tissue. C57BL/6 mice were subjected to sham-operation (sham), saline treatment, and liver ischemia and reperfusion (IR) or APC treatment during and after liver IR (APC + IR). The kidneys were obtained 5 h after reperfusion. (**b**) Densitometric quantification of relative MCP-1 and MIP-2 band intensities normalized to GAPDH from RT-PCRs. Data are presented as means ± s.e.m. $^{*}P<0.05$ vs sham group. $^{\#}P<0.05$ vs IR group.

TNF-α mRNA in the liver and MCP-1 and MIP-2 mRNA in the kidney compared with the saline-treated mice at 5 h (Figures 6 and 7) and at 24 h (data not shown) after liver IR. There were no significant differences in other pro-inflammatory mRNAs. Inhibition of PAR-1 with SCH 79797 (0.5 mg/kg i.p.) 1 h before APC treatment (250 μg/kg i.v. before reperfusion and 500 μg/kg s.c. 2 h after reperfusion) prevented the reduction of TNF-α mRNA in the liver and MCP-1 and MIP-2 mRNA in the kidney at 5 h and at 24 h after liver IR (data not shown).

APC treatment reduces hepatic and renal apoptosis after liver IR

We used three separate indices to detect apoptosis: TUNEL staining, DNA laddering, and caspase 3 fragmentation. APC treatment significantly reduced the apoptosis of the liver and kidney compared with the saline-treated mice with reduced TUNEL staining (Figure 8), DNA laddering (Figure 9), and caspase 3 fragmentation (Figure 10). The TUNEL staining showed that endothelial apoptosis was predominant in the kidney (Figure 8b inset).

APC treatment reduces the degradation of hepatic and renal F-actin after liver IR

Liver staining in sham-operated mice shows localization of F-actin at the hepatocyte basolateral membranes and the bile canalicular membranes (Figure 11a). As expected, 60 min of liver ischemia and 24 h of reperfusion resulted in severe disruption of liver parenchymal F-actin compared with the sham-operated mice (Figure 11a, representative of six experiments) in saline-treated mice as the staining of basolateral hepatocyte membranes as well as bile canalicular

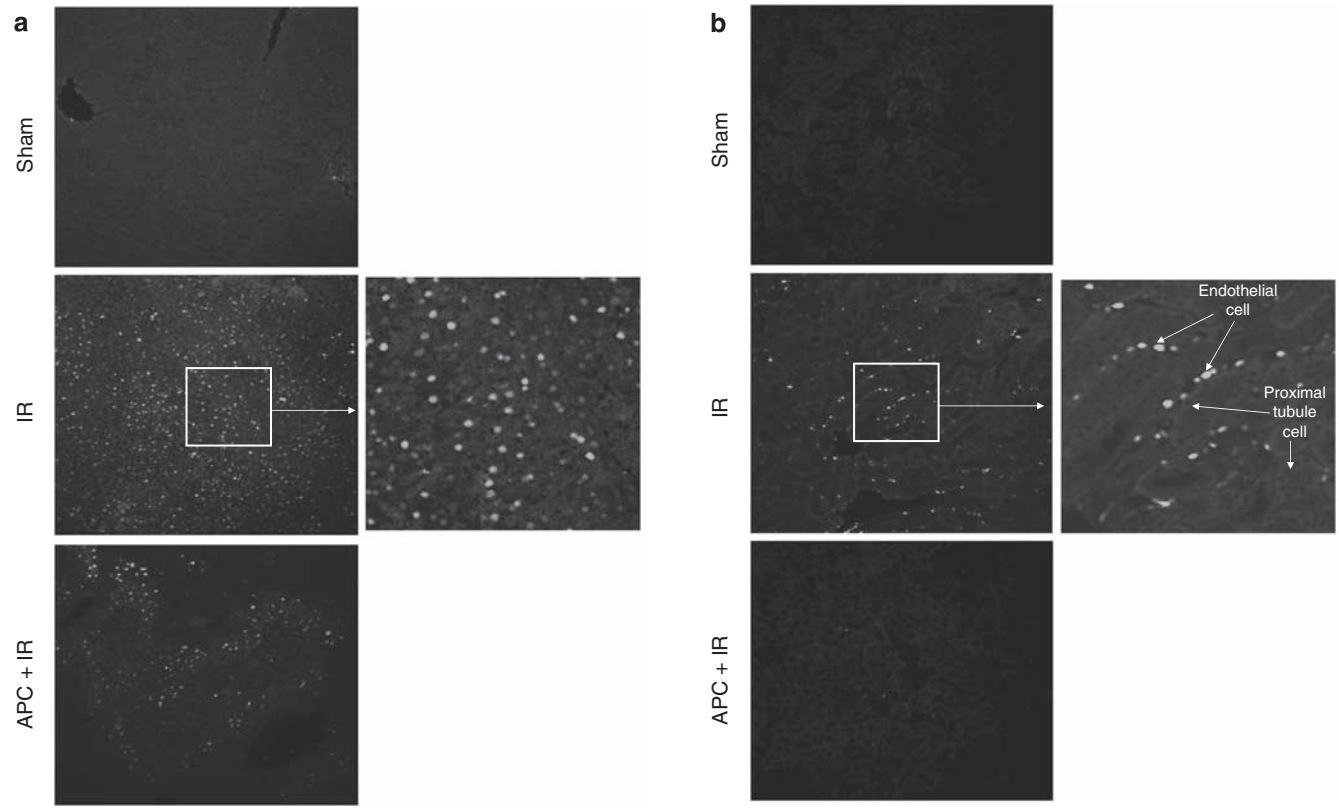

Figure 8 | Representative fluorescent photomicrographs of liver and kidney sections illustrate apoptotic nuclei (TUNEL fluorescent stain, magnification ×100). C57BL/6 mice were subjected to sham operation (sham), saline treatment, and liver ischemia and reperfusion (IR) or APC treatment during and after liver IR (APC + IR). The liver (**a**) and kidney (**b**) sections were obtained 24 h after reperfusion. Photographs are representative of six independent experiments. Insets show a higher magnification of the images showing TUNEL positive cells. In the kidney, endothelial cells and not proximal tubule cells underwent apoptosis.

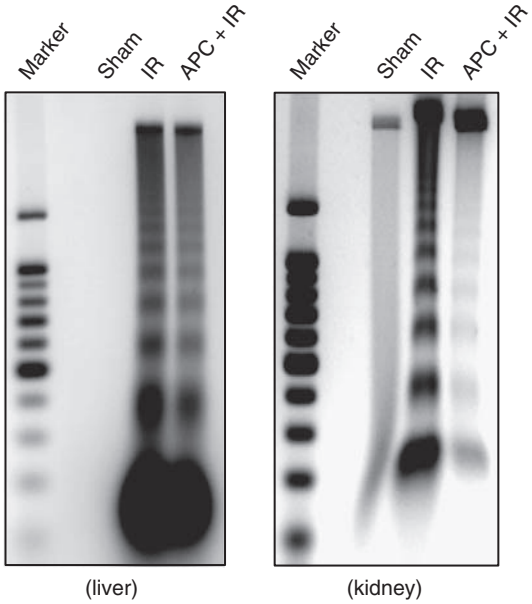

Figure 9 | Representative gel images demonstrating DNA laddering as an index of DNA fragmentations in the liver and kidney tissues. C57BL/6 mice were subjected to sham operation (sham), saline treatment, and liver ischemia and reperfusion (IR) or APC treatment during and after liver IR (APC + IR). The liver and kidney tissues were obtained 24 h after reperfusion. Photographs are representative of five independent experiments.

membranes is strongly decreased and disorganized. However, APC-treated mice subjected to liver IR show significantly better preserved F-actin structure after liver IR as the staining is quite similar to that of sham-operated mice. Liver IR also resulted in a severe loss of F-actin in renal proximal tubules in 24 h. In Figure 11a, 24 h post-hepatic IR-induced disruptions of the F-actin cytoskeleton in renal proximal tubular epithelial cells are also shown. Mice subjected to sham surgery showed intense stain in the tubular epithelial and in the basal plasma membrane. In contrast, kidneys from saline-treated mice subjected to liver IR showed loss of F-actin staining in the tubular epithelial cells. However, the APC-treated mice show significantly better preserved F-actin structure after liver IR as the staining is quite similar to that of sham-operated mice. Mean fluorescent F-actin intensity showed reduced hepatocyte and renal proximal tubule F-actin degradation in APC-treated mice after liver IR (Figure 11b).

DISCUSSION

The major findings of this study are that mice treated with human APC show reduced hepatic and renal injury after liver IR, which was reversed by pretreatment with the PAR-1 antagonist SCH 79797. APC-treated mice subjected to liver IR show (1) reduced hepatic and renal necrosis as well as

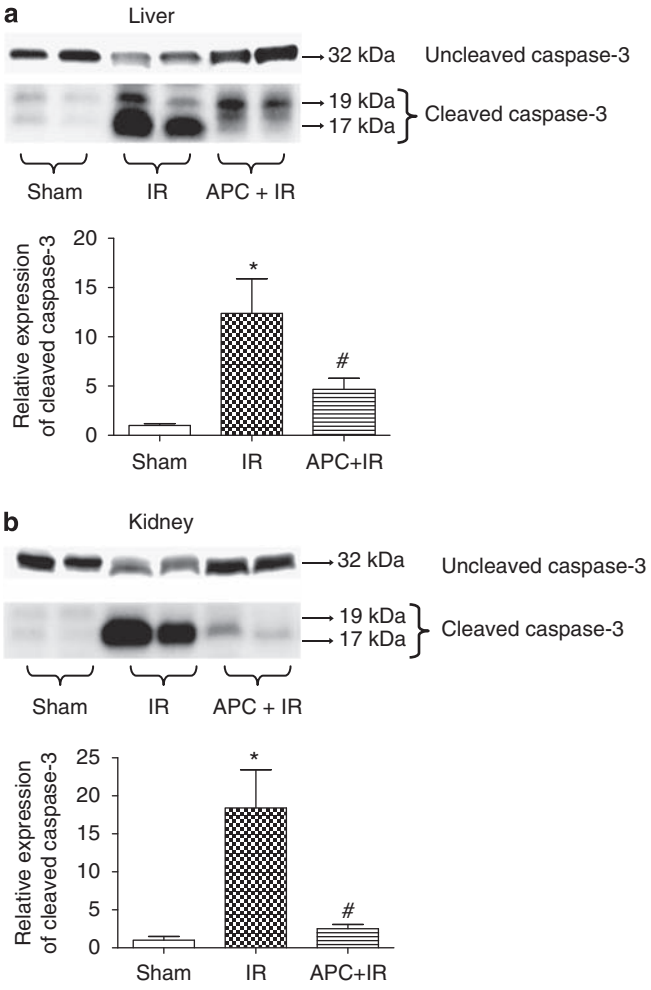

Figure 10 | Effect of APC on caspase 3 fragmentation after hepatic IR. Top: representative caspase 3 fragmentation in liver (**a**) and kidney (**b**) tissues. C57BL/6 mice were subjected to sham operation (sham), saline treatment, and liver ischemia and reperfusion (IR) or APC treatment during and after liver IR (APC + IR). The liver and kidney tissues were obtained 24 h after reperfusion. Photographs are representative of four independent experiments. Bottom: densitometric quantifications of cleaved caspase 3 (pro-caspase 3) mice subjected to sham operation or liver IR ($N = 4$ for each group). $^{*}P < 0.05$ vs sham group. $^{\#}P < 0.05$ vs IR group.

apoptosis, (2) decreased neutrophil infiltration of the kidney, (3) improved vascular permeability indicating better preserved endothelial integrity of the liver and the kidney, (4) attenuated expression of certain pro-inflammatory mRNAs in the liver and the kidney and a reduction in plasma TNF-α levels and (5) better preserved F-actin cytoskeleton structure after liver IR.

Hepatic IR-induced acute liver dysfunction is a very common clinical problem and frequently complicates several surgical procedures including major liver resection, procedures requiring prolonged portal vein occlusion and orthotopic liver transplantation.[15] Unfortunately, neither effective prevention nor therapy exists for hepatic IR-induced liver dysfunction and the current management remains largely supportive.[2] Furthermore, hepatic IR is also known to cause remote organ injury resulting in myocardial dysfunction, pulmonary failure, and AKI.[3,5] In particular, AKI associated with liver failure is a grave clinical problem with a high mortality rate.[16] Therapy for AKI also remains largely supportive and limited to hydration, blood pressure support and short-term hemodialysis until renal function recovers.

In human liver transplantation surgery involving obligatory prolonged liver ischemia, severe inflammatory responses during reperfusion may lead to protein C and APC utilization within the liver leading to systemic depletion.[17] Therefore, we hypothesized that an exogenous supply of APC would protect against the detrimental effects of liver IR and attenuate remote kidney injury associated with liver IR. In this study, hepatic IR-induced severe hepatocellular damage resulting in a dramatic elevation of plasma ALT level at 5 and 24 h of reperfusion. Moreover, liver IR also caused subsequent AKI during the late phase of reperfusion (24 h). APC treatment significantly attenuated the elevation of plasma ALT and creatinine levels. Therefore, these results show that APC has a protective effect against liver as well as kidney injury caused by hepatic IR.

Protein C produces three distinct but perhaps interrelated physiological effects.[18] It is one of the main physiological vitamin K-dependent anticoagulants in the blood. Upon activation by thrombin–thrombomodulin complex at the endothelial surface, it is converted to an active form of the serine protease, APC.[19] APC produces anticoagulant activity by inhibiting thrombin generation by selective proteolytic inactivation of factors Va and VIIIa and stimulates fibrinolysis by diminishing thrombin generation with subsequent reduction in thrombin-dependent PAR-1 cleavage. In addition, APC is a powerful endogenous cytoprotective agent with anti-inflammatory and antiapoptotic properties. Furthermore, APC attenuates the activation of leukocytes and suppresses cytokine production.[20] APC's cytoprotective effects are secondary to endothelial protein C receptor activation with subsequent cleavage of protease-activated receptor-1.[18] Finally, APC may reduce neutrophil migration via PAR-1 independent mechanisms, thereby also reducing inflammation. All of these physiological effects of APC (anticoagulant, antiapoptotic, anti-inflammatory, endothelial protection) are perfectly suited to attenuate the detrimental effects of liver IR and subsequent remote kidney injury. Indeed, APC infusion or injection has been shown to protect against liver injury after hepatectomy[21] and in animals subjected to endotoxemia[22] and peritonitis.[23] However, the protective effect of APC on renal function after hepatic IR injury has never been described. Utilization of APC to treat AKI associated with liver IR is particularly exciting as we saw changes in the kidney after liver IR that may be mitigated by APC (endothelial apoptosis, tubular inflammation and apoptosis, and F-actin degradation).[5] Therefore, we examined in this study whether APC treatment has a protective

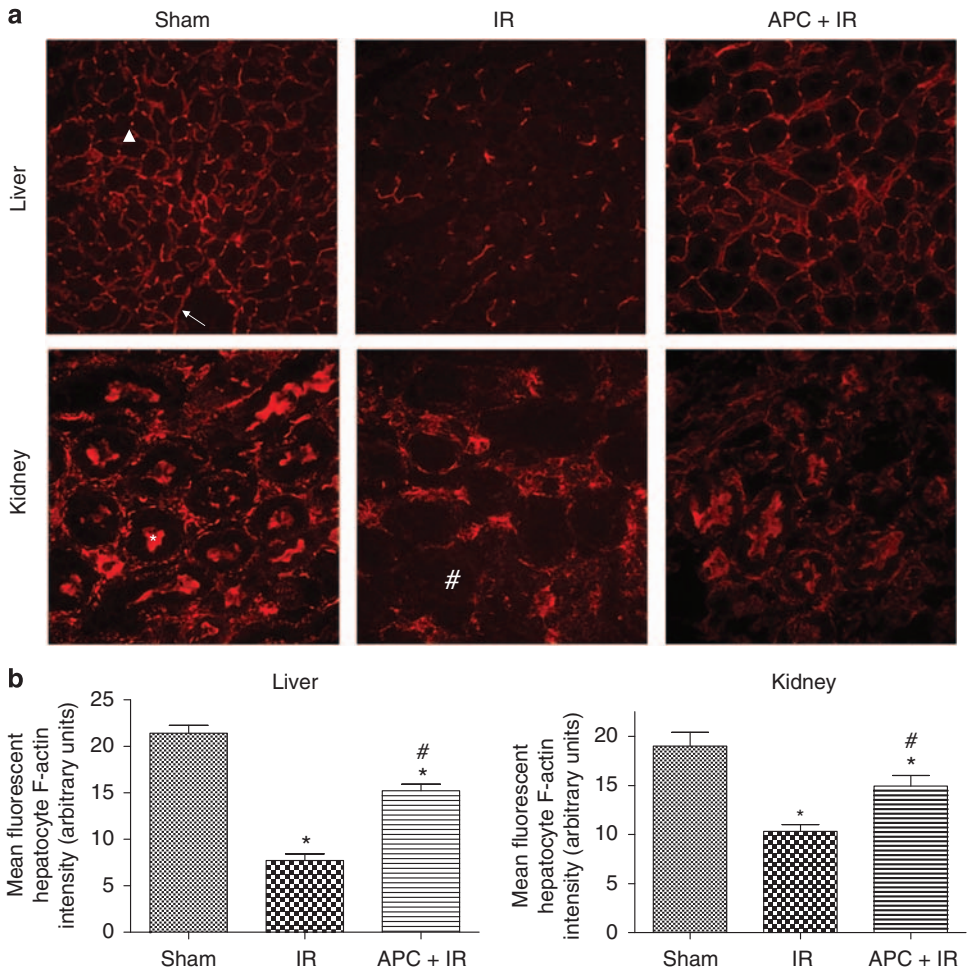

Figure 11 | Effect of APC on F-actin degradation after hepatic IR. (**a**) Representative fluorescent photomicrographs of phalloidin staining of the liver and kidney tissues (magnification ×400). C57BL/6 mice were subjected to sham operation (sham), saline treatment, and liver ischemia and reperfusion (IR) or APC treatment during and after liver IR (APC + IR). The liver and kidney sections were obtained 24 h after reperfusion. In the liver, F-actin is localized in basolateral membranes (arrow) and bile canalicular membranes. Transverse sections of bile canaliculi are seen as typical dots (arrowhead). In the kidney, F-actin stains of proximal tubular epithelial cells are prominent in the brush border from sham-operated mice (*), which is severely degraded in the kidneys of mice subjected to liver IR (#). Photographs are representative of six independent experiments. (**b**) Quantification of mean fluorescent hepatocyte ($N = 6$) and renal proximal tubule ($N = 6$) F-actin intensity. $^{*}P < 0.05$ vs sham group. $^{\#}P < 0.05$ vs IR group.

effect against hepatic as well as renal injury that occur after liver IR. We demonstrated in this study that a selective PAR-1 receptor antagonist (SCH 79797) dose-dependently inhibited APC's protective effects against liver and kidney injury after liver IR. SCH 79797 also blocked the reduction in TNF-α mRNA in the liver and MCP-1 and MIP-2 mRNA in the kidney induced by APC treatment after liver IR. Therefore, we conclude that the cytoprotective effects of APC against liver IR is due to PAR-1 modulation. Although dose-dependent inhibition of APC was provided by the PAR-1 antagonist, we also noticed that an intermediate dose of this PAR-1 antagonist (0.1 mg/kg SCH 79797) produced moderate hepatic (but not renal) protection after liver IR. After myocardial IR in rats, this PAR-1 antagonist also provided protection.[24]

In this study, we demonstrate that APC treatment significantly reduced the necrosis of liver parenchyma as well as renal proximal tubules after liver IR. Necrotic liver cell death occurs directly by total breakdown of cellular homeostatic machinery secondary to massive depletion of ATP during and after the ischemic period. Necrosis can also occur during reperfusion where uncontrolled delivery of cytotoxic cytokines or free radicals cause further cellular derangements.[25] We also demonstrate that APC treatment also suppress apoptotic cell death of the liver and the kidney after liver IR (reduced TUNEL staining, DNA laddering, caspase 3 fragmentation). Apoptosis is an important contributor in the development of liver failure after IR.[26] Apoptotic cell death represents the execution of an ATP-dependent death program often initiated by death ligand/death receptor interactions, such as Fas ligand with Fas, which leads to a caspase 3 activation and cleavage of DNA and the DNA-reparative enzyme poly (ADP-ribose) polymerase (PARP).[27] APC was able to reduce both hepatic as

well as renal apoptosis. Although we saw global apoptotic changes in the liver after IR, the pattern of apoptosis in the kidney after liver IR was unique (and different compared with the pattern observed after renal IR) in that endothelial apoptosis predominated (Figure 8b and Lee *et al.*[5]). We propose that protection of renal endothelial apoptosis is a crucial mechanism of renal protection with APC after hepatic IR. Reduction in renal endothelial apoptosis would lead to better preserved vascular permeability, reduced neutrophil infiltration with subsequently reduced proximal tubule cell death. All of these changes were observed in the kidneys of APC-treated mice subjected to liver IR.

We used a model of AKI in mice induced with liver IR that is reproducible, rapid to develop (in less than 24 h) and mimics the histological (renal tubular damage, apoptosis, necrosis, and juxtaglomerular apparatus hyperplasia) as well as biochemical (plasma creatinine, inflammatory markers) changes observed with human AKI associated with liver failure.[5] The pathophysiological and biochemical mechanisms of AKI associated with liver IR appear to be multifactorial involving portal hypertension-induced splanchnic vasodilatation with subsequent intrarenal vasoconstriction[28–30] coupled with a systemic inflammatory response after liver IR.[30,31] After liver IR injury, circulating pro-inflammatory cytokines including TNF-α increase significantly.[32] We determined in this study that plasma TNF-α levels increased significantly after liver IR and APC treatment attenuated this increase, which may have contributed to the reduction in the degree of AKI after liver IR.

The production of several pro-inflammatory cytokines and adhesion molecules after hepatic IR contributes to the pathophysiology of liver injury.[1,33] We demonstrate that as expected, all of the pro-inflammatory mRNAs examined in the liver (TNF-α, KC, MCP-1, MIP-2, and ICAM-1) show enhanced expression after hepatic IR. However, we only saw reductions in TNF-α mRNA after liver IR in mice treated with APC. This attenuation in TNF-α mRNA is consistent with a significant reduction in plasma TNF-α protein levels detected with ELISA. We also measured the pro-inflammatory mRNA expression in the kidney after liver IR and similar to the liver, we saw drastic increases in the expression of several pro-inflammatory mRNAs. However, we saw significant reductions in the expression of only two pro-inflammatory mRNAs (MIP-2 and MCP-1) in APC-treated mice. The CC chemokine MCP-1 and CXC chemokine MIP-2 are important mediators in the pathogenesis of AKI.[34] Upregulation of MCP-1 and MIP-2 leads to neutrophil recruitment during AKI induced by renal IR or nephrotoxic agents.[35] APC may have directly but selectively attenuated the MIP-2 and MCP-1 expression in the kidney, but more likely, the reduction in hepatic TNF-α expression with APC treatment resulted in a secondary reduction in MIP-2 and MCP-1 expression in the kidney. Moreover, TNF-α is known to promote the migration of inflammatory cells into the renal parenchyma via the upregulation of MCP-1 and MIP-2 in the kidney.[36]

The role of neutrophils in the pathophysiology of organ injury (including the liver and the kidney) is well recognized.[37] Our study demonstrated that liver IR not only caused rapid infiltration of neutrophils in the liver but also caused neutrophil infiltration in the kidney. Neutrophils are activated during and after liver ischemia and activated neutrophils attach to and then transverse the hepatic capillary endothelium into the subendothelial space, where they release enzymes and cytokines, causing direct hepatocyte injury and recruit other injurious cells, such as monocytes and macrophages.[38,39] Activated neutrophils release substances to produce further tissue injury such as products of arachidonic acid metabolism, oxygen-free radicals and neutrophil elastase.[37] Treating mice with APC resulted in improved kidney vascular endothelial integrity (indicated by reduced EBD infiltration) which most likely was responsible for the limited PMN infiltration into the kidney.

Ischemia-reperfusion injury *in vivo* results in F-actin cytoskeleton degradation, which further compromises organ function.[40,41] For example, F-actin disruption is a well known stimulus of apoptosis in several cell lines.[42] We saw severe disruption of F-actin in the liver as well as in the kidney proximal tubules after liver IR in saline-treated mice. Specifically, we saw severe disruptions in both hepatocyte and bile canalicular F-actin cytoskeleton after liver IR (Figure 11). Remarkably, proximal tubule brush border F-actin was completely disrupted after liver IR (Figure 11). In this study, we showed that APC treatment resulted in markedly better preserved F-actin in the liver as well as the kidney. Preservation of an intact F-actin cytoskeleton in the liver and the kidney of mice subjected to liver IR may have contributed to reduced necrosis and apoptosis observed in these mice.

APC produces dual effects *in vivo*; anticoagulant or cytoprotective. Clinical APC therapy may be limited by its anticoagulant properties with increased risk of bleeding. In fact, an increased risk of bleeding has been observed in clinical trials (PROWESS trial),[43] although, in this study the mice subjected to major laparotomy and liver ischemia well-tolerated the APC injections. Several APC variants with varying antithrombotic and cytoprotective activities have been designed.[44,45] In fact, Gupta *et al.*[46] generated APC variants to study the relative contributions of the two functions of APC in a rat model of LPS-induced renovascular dysfunction. In their study, they used two variants of wild-type APC: K193E (a variant with impaired anticoagulant activity with intact PAR-1-dependent signaling) and L8W (a variant with normal anticoagulant activity without the ability to modulate PAR-1). They determined that the PAR-1 modulation without the anticoagulant function of APC reversed LPS-induced hypotension. In contrast, both functions of APC had a role in reversing LPS-induced decreases in renal blood flow and volume to have distinct roles in attenuating the response to injury in the kidney. In our model of APC-mediated kidney and liver protection, the cytoprotective signaling is through agonism of the PAR-1

receptor as inhibition of PAR-1 with SCH 79797 blocked the protective effects of APC.

Our model of liver IR-induced AKI demonstrates that the plasma ALT and Cr has a direct and linear relationship: mice with higher ALT showed increased renal dysfunction after liver IR. We also noted that the degree of renal dysfunction was mild when the plasma ALT levels were below 10,000 U/l.[5] In the study by Behrends *et al.*,[3] rats subjected to 75 min of partial liver IR developed acute liver dysfunction at 24 h. However, the degree of renal dysfunction in their rat model was mild with modest increases in plasma creatinine, upregulation of ICAM-1 mRNA expression but no changes in renal MCP-1, MIP2, and iNOS expression. Furthermore, the kidneys from rats subjected to liver IR showed little morphological damage and they failed to see increases in apoptosis (caspase-3) and neutrophil infiltration (myeloperoxidase activity). The reason for this discrepancy between our mouse model and the previous rat model is unclear but is likely related to differences in the severity of liver injury which in turn influences the degree of kidney injury. In the study by Behrends *et al.*[3] plasma ALT rose only to ~6800 U/l whereas in our mouse model, the plasma ALT rose much higher (~15–2,0000 U/l). Longer liver ischemic period (for example, 90 min) in a rat is usually lethal (unpublished observations). Therefore, it appears that the murine model is better suited as a model of liver failure-induced AKI than the rat model.

In conclusion, this is the first study to demonstrate the protective effects of APC on both hepatic and renal dysfunction induced with hepatic IR injury. Our study shows that APC attenuates both hepatic and renal injury after liver IR by reducing necrosis, inflammation, and apoptosis of both organs. APC treatment led to better preserved F-actin cytoskeleton and improved vascular integrity of the liver as well as the kidney after liver IR. Moreover, APC treatment reduced neutrophil infiltration into the kidney after liver IR. Therefore, the APC-signaling pathway may be considered as a promising pharmacological strategy for protecting both liver and kidney function during and after hepatic IR.

MATERIALS AND METHODS

Reagents

Human APC was purchased from Haematologic Technologies (Essex Junction, VT, USA). Unless otherwise specified, all reagents were purchased from Sigma (St. Louis, MO, USA).

Murine model of hepatic IR

All protocols were approved by the Institutional Animal Care and Use Committee of Columbia University. Male C57BL/6 mice (20–25 g, Harlan, Indianapolis, IN, USA) were subjected to liver IR injury as described previously.[5] This method of partial hepatic ischemia results in a segmental (~70%) hepatic ischemia but spares the right lobe of the liver and prevents mesenteric venous congestion by allowing portal decompression through the right and caudate lobes of the liver. Sham-operated mice were subjected to laparotomy and identical liver manipulations without the vascular occlusion. Human APC or saline vehicle was injected intravenously (i.v.) before reperfusion and then subcutaneously (s.c.) 2 h after reperfusion. Three doses of APC were given to mice: 40, 100, or 250 μg/kg i.v. prior to reperfusion and 80, 200 or 500 μg/kg s.c. 2 h after reperfusion. Preliminary data showed that APC injection alone in sham-operated mice had no effect on any of the injury parameters tested in the liver or in the kidney. Twenty-four hours after reperfusion, the liver tissue subjected to IR and kidney were collected to measure necrosis, neutrophil infiltration (with immunohistochemistry), vascular permeability, apoptosis (with terminal deoxynucleotidyl transferase-mediated dUTP nick end-labeling staining, DNA laddering and caspase 3 protein cleavage), and F-actin integrity. In some mice, liver and kidney were collected at 5 h and at 24 h after reperfusion to detect inflammatory changes by RT-PCR for pro-inflammatory cytokine mRNAs. We also collected plasma for the measurement of alanine aminotransferase (ALT) and creatinine at 5 and 24 h after reperfusion. Plasma levels of tumor necrosis factor (TNF)-α were measured 24 h after reperfusion.

To test whether the blockade of PAR-1 would prevent the renal and hepatic protective effects of APC after liver IR, we pretreated mice with SCH 79797 (0.02–0.5 mg/kg i.p.), a selective non-peptide antagonist for PAR-1 30 min before APC administration (250 μg/kg i.v. before reperfusion and 500 μg/kg s.c. 2 h after reperfusion) in mice subjected to liver IR.

Plasma ALT activity and creatinine level

The plasma and urine ALT activities were measured using the Infinity ALT assay kit according to the manufacturer's instructions (Thermo Fisher Scientific, Waltham, MA, USA). Plasma creatinine was measured by a colorimetric method based on the Jaffe reaction.[47]

Histological analysis of hepatic and renal injury

For histological preparations, liver or kidney tissues were fixed in 10% formalin solution overnight. After automated dehydration through a graded alcohol series, transverse liver slices were embedded in paraffin, sectioned at 5 μm, and stained with hematoxylin–eosin (H&E). To quantify the degree of hepatic necrosis, H&E stains were digitally photographed and the percent of necrotic area was quantified with NIH IMAGE (Image-J, 1.37v) software by a person (SWC) who was blinded to the treatment each animal had received. Twenty random sections were investigated per slide to determine the percentage of necrotic area. Liver H&E sections were also graded for IR injury by a pathologist (VDD) blinded to the samples using the system devised by Suzuki *et al.*[14] In this classification, three liver injury indices are graded: sinusoidal congestion (0–4), hepatocyte necrosis (0–4), and ballooning degeneration (0–4) are graded for a total score of 0–12. No necrosis, congestion, or centrilobular ballooning is given a score of 0 whereas severe congestion/ballooning and >60% lobular necrosis is given a value of four. Renal H&E sections were evaluated for renal cortical vacuolization, proximal tubule simplification, and proximal tubule hypereosinophilia by an experienced pathologist (VDD) who was blinded to the treatment each animal had received.

Assessment of liver and kidney inflammation

Liver and kidney inflammation after hepatic ischemia was determined with detection of neutrophil infiltration by immunohistochemistry (Serotec Clone 7/4 at 1:200 concentration for primary and a biotin-conjugated secondary, rabbit anti-rat at 1:100 concentration) 24 h after hepatic IR as described previously[48]

Table 1 | RT-PCR primers used in this study

Genes	Species	Amplicon size (bp)	Primer sequences (sense/antisense)	Annealing °C/cycle no.
GAPDH	Mouse	450	5′-ACCACAGTCCATGCCATCAC-3′ 5′-CACCACCCTGTTGCTGTAGCC-3′	65/15
TNF-α	Mouse	290	5′-TACTGAACTTCGGGGTGATTGGTCC-3′ 5′-CAGCCTTGTCCCTTGAAGAGAACC-3′	65/24
ICAM-1	Mouse	409	5′-TGTTTCCTGCCTCTGAAGC-3′ 5′-CTTCGTTTGTGATCCTCCG-3′	60/21
KC	Mouse	203	5′-CAATGAGCTGCGCTGTCAGTG-3′ 5′-CTTGGGGACACCTTTTAGCATC-3′	60/26
MCP-1	Mouse	312	5′-ACCTGCTGCTACTCATTCAC3-′ 5′-TTGAGGTGGTTGTGGAAAAG3-′	60/22
MIP-2	Mouse	282	5′-CCAAGGGTTGACTTCAAGAAC-3′ 5′-AGCGAGGCACATCAGGTACG-3′	60/25

GAPDH, glyceraldehyde 3-phosphate dehydrogenase; ICAM-1, intercellular adhesion molecule-1; KC, keratinocyte-derived chemokine, MCP-1, monocyte chemoattractant protein 1, MIP-2, macrophage inflammatory protein 2, TNFα, tumor necrosis factor alpha.

and by measuring mRNA-encoding markers of inflammation, including keratinocyte-derived cytokine (KC), intercellular adhesion molecule-1 (ICAM-1), monocyte chemoattractive protein-1 (MCP-1), macrophage inflammatory protein-2 (MIP-2), and TNF-α 5 h after liver IR (Table 1). RT-PCR were performed as described.[5]

Vascular permeability of liver and kidney tissues

Changes in liver and kidney vascular permeability were assessed by quantitating extravasation of Evans blue dye (EBD) into the tissue as described by Awad *et al.*[49] with some modifications. Briefly, 2% EBD (Sigma Biosciences, St. Louis, MO, USA) was administered intravenously at a dose of 20 mg/kg 24 h after liver injury. One hour later, mice were killed and perfused through the heart with PBS and EDTA with 10 ml cold saline with heparin (100 U/ml). Liver and kidneys were then removed, allowed to dry overnight at 60 °C, and the dry weights were determined. EBD was extracted in formamide (20 ml/g dry tissue; Sigma Biosciences), homogenized, and incubated at 60 °C overnight. Homogenized samples were centrifuged at 12,000 *g* for 30 min and the supernatants were measured at 620 and 740 nm in a spectrophotometer. The extravasated EBD concentration was calculated against a standard curve and the data expressed as micrograms of EBD per gram of dry tissue weight.

Enzyme-linked immunosorbent assay for plasma TNF-α

Twenty-four hours after reperfusion, the plasma TNF-α level was measured by the mouse TNF-α ELISA kit according to the manufacturer's instruction (eBiosciences, San Diego, CA, USA).

Detection of liver and kidney apoptosis

We used three independent assays to assess the degree of liver and kidney apoptosis after IR: with *in situ* Terminal Deoxynucleotidyl Transferase Biotin-dUTP Nick End-Labeling (TUNEL) assay, detection of DNA laddering and immunoblotting for fragmented caspase 3. For DNA laddering, liver and kidney tissues were removed 24 h after liver IR, apoptotic DNA fragments were extracted according to the methods of Herrmann *et al.*[50] and was electrophoresed at 70 V in a 2.0% agarose gel in Tris-acetate–EDTA buffer. This method of DNA extraction selectively isolates apoptotic, fragmented DNA and leaves behind the intact chromatin. The gel was stained with ethidium bromide and photographed under UV illumination. DNA ladder markers (100 bp) were added to a lane of each gel as a reference for the analysis of internucleosomal DNA fragmentation. For the TUNEL assay, fixed liver, and kidney sections obtained at 24 h after hepatic IR were deparaffinized in xylene and rehydrated through graded ethanols to water. *In situ* TUNEL staining was used for detecting DNA fragmentation in apoptosis using a commercially available *in situ* cell death detection kit (Roche, Nutley, NJ, USA) according to the manufacturer's instructions. Caspase 3 immunoblotting was performed as described previously.[5]

F-actin staining of liver and kidney sections

As breakdown of F-actin occurs early after IR, we visualized the F-actin cytoskeleton by staining with phalloidin as an early index of liver as well as renal injury.[51] Twenty-four hours after hepatic IR, liver and kidney tissues were embedded in Tissue-Tek oxytetracycline compound (Fisher Scientific, Pittsburgh, PA, USA) and cut into 5 μm sections. To reduce background staining, the sections were incubated in 1% BSA dissolved in PBS for 10 min at room temperature. The sections were then stained with Alexafluor 594 (Red)-labeled phalloidin (Invitrogen, Carlsbad, CA, USA) for 30 min at 37 °C in a humidified chamber in the dark. Sections were then washed twice in PBS and mounted with Vectashield (Vector Laboratories, Burlingame, CA, USA). F-actin images were visualized with an Olympus IX81 epifluorescence microscope (Tokyo, Japan) and captured and stored using SlideBook 4.2 software (Intelligent Imaging Innovations Inc., Denver, CO, USA) on a personal computer.

Protein determination

Protein contents were determined with a bicinchoninic acid protein assay kit (Pierce Chemical Co., Rockford, IL, USA), using bovine serum albumin as a standard.

Statistical analysis

All data are reported as mean ± s.e. The overall significance of the results was examined using one-way analysis of variance and the significant differences between the groups were considered at a $P<0.05$ with the appropriate Tukey's *post hoc* test made for multiple comparisons. Twenty-four hours survival rates between vehicle hepatic IR and APC hepatic IR groups were compared with χ^2-test.

DISCLOSURE

All the authors declared no competing interests.

REFERENCES

1. Serracino-Inglott F, Habib NA, Mathie RT. Hepatic ischemia-reperfusion injury. *Am J Surg* 2001; **181**: 160–166.
2. Fondevila C, Busuttil RW, Kupiec-Weglinski JW. Hepatic ischemia/reperfusion injury—a fresh look. *Exp Mol Pathol* 2003; **74**: 86–93.
3. Behrends M, Hirose R, Park YH *et al.* Remote renal injury following partial hepatic ischemia/reperfusion injury in rats. *J Gastrointest Surg* 2008; **12**: 490–495.
4. Weinbroum AA, Hochhauser E, Rudick V *et al.* Direct induction of acute lung and myocardial dysfunction by liver ischemia and reperfusion. *J Trauma* 1997; **43**: 627–633.
5. Lee HT, Park SW, Kim M *et al.* Acute kidney injury after hepatic ischemia and reperfusion injury in mice. *Lab Invest* 2009; **89**: 196–208.
6. Esmon CT. The protein C pathway. *Chest* 2003; **124**: 26S–32S.
7. Mosnier LO, Griffin JH. Protein C anticoagulant activity in relation to anti-inflammatory and anti-apoptotic activities. *Front Biosci* 2006; **11**: 2381–2399.
8. Bartolome S, Wood JG, Casillan AJ *et al.* Activated protein C attenuates microvascular injury during systemic hypoxia. *Shock* 2008; **29**: 384–387.
9. Sharfuddin AA, Sandoval RM, Berg DT *et al.* Soluble thrombomodulin protects ischemic kidneys. *J Am Soc Nephrol* 2009; **20**: 524–534.
10. Bernard GR, Vincent JL, Laterre PF *et al.* Efficacy and safety of recombinant human activated protein C for severe sepsis. *N Engl J Med* 2001; **344**: 699–709.
11. Yesilirmak DC, Kumral A, Tugyan K *et al.* Effects of activated protein C on neonatal hypoxic ischemic brain injury. *Brain Res* 2008; **1210**: 56–62.
12. Pirat B, Muderrisoglu H, Ual MT *et al.* Recombinant human-activated protein C inhibits cardiomyocyte apoptosis in a rat model of myocardial ischemia-reperfusion. *Coron Artery Dis* 2007; **18**: 61–66.
13. Teke Z, Sacar M, Yenisey C *et al.* Activated protein C attenuates intestinal mucosal injury after mesenteric ischemia/reperfusion. *J Surg Res* 2008; **149**: 219–230.
14. Suzuki S, Toledo-Pereyra LH, Rodriguez FJ *et al.* Neutrophil infiltration as an important factor in liver ischemia and reperfusion injury. Modulating effects of FK506 and cyclosporine. *Transplantation* 1993; **55**: 1265–1272.
15. Montalvo-Jave EE, Escalante-Tattersfield T, Ortega-Salgado JA *et al.* Factors in the pathophysiology of the liver ischemia-reperfusion injury. *J Surg Res* 2008; **147**: 153–159.
16. Biancofiore G, Davis CL. Renal dysfunction in the perioperative liver transplant period. *Curr Opin Organ Transplant* 2008; **13**: 291–297.
17. Ilmakunnas M, Pesonen EJ, Hockerstedt K *et al.* Graft protein C entrapment is associated with reduced phagocyte activation during reperfusion in human liver transplantation. *Crit Care Med* 2006; **34**: 426–432.
18. Slofstra SH, ten CH, Spek CA. Signal transduction induced by activated protein C: no role in protection against sepsis? *Trends Mol Med* 2006; **12**: 374–381.
19. Vu TK, Hung DT, Wheaton VI *et al.* Molecular cloning of a functional thrombin receptor reveals a novel proteolytic mechanism of receptor activation. *Cell* 1991; **64**: 1057–1068.
20. Dillon JP, Laing AJ, Cahill RA *et al.* Activated protein C attenuates acute ischaemia reperfusion injury in skeletal muscle. *J Orthop Res* 2005; **23**: 1454–1459.
21. Yoshikawa A, Kaido T, Seto S *et al.* Activated protein C prevents multiple organ injury following extensive hepatectomy in cirrhotic rats. *J Hepatol* 2000; **33**: 953–960.
22. Lehmann C, Meissner K, Knock A *et al.* Activated protein C improves intestinal microcirculation in experimental endotoxaemia in the rat. *Crit Care* 2006; **10**: R157.
23. van Veen SQ, Levi M, van Vliet AK *et al.* Peritoneal lavage with activated protein C alters compartmentalized coagulation and fibrinolysis and improves survival in polymicrobial peritonitis. *Crit Care Med* 2006; **34**: 2799–2805.
24. Strande JL, Hsu A, Su J *et al.* SCH 79797, a selective PAR1 antagonist, limits myocardial ischemia/reperfusion injury in rat hearts. *Basic Res Cardiol* 2007; **102**: 350–358.
25. Saikumar P, Dong Z, Weinberg JM *et al.* Mechanisms of cell death in hypoxia/reoxygenation injury. *Oncogene* 1998; **17**: 3341–3349.
26. Daemen MA, de Vries B, Buurman WA. Apoptosis and inflammation in renal reperfusion injury. *Transplantation* 2002; **73**: 1693–1700.
27. Lieberthal W, Koh JS, Levine JS. Necrosis and apoptosis in acute renal failure. *Semin Nephrol* 1998; **18**: 505–518.
28. Wadei HM, Mai ML, Ahsan N *et al.* Hepatorenal syndrome: pathophysiology and management. *Clin J Am Soc Nephrol* 2006; **1**: 1066–1079.
29. Schepke M. Hepatorenal syndrome: current diagnostic and therapeutic concepts. *Nephrol Dial Transplant* 2007; **22**(Suppl 8): viii2–viii4.
30. Davis CL, Gonwa TA, Wilkinson AH. Pathophysiology of renal disease associated with liver disorders: implications for liver transplantation. Part I. *Liver Transpl* 2002; **8**: 91–109.
31. Tanaka Y, Maher JM, Chen C *et al.* Hepatic ischemia-reperfusion induces renal heme oxygenase-1 via NF-E2-related factor 2 in rats and mice. *Mol Pharmacol* 2007; **71**: 817–825.
32. Wanner GA, Ertel W, Muller P *et al.* Liver ischemia and reperfusion induces a systemic inflammatory response through Kupffer cell activation. *Shock* 1996; **5**: 34–40.
33. Frangogiannis NG. Chemokines in ischemia and reperfusion. *Thromb Haemost* 2007; **97**: 738–747.
34. Furuichi K, Wada T, Iwata Y *et al.* CCR2 signaling contributes to ischemia-reperfusion injury in kidney. *J Am Soc Nephrol* 2003; **14**: 2503–2515.
35. Miura M, Fu X, Zhang QW *et al.* Neutralization of Gro alpha and macrophage inflammatory protein-2 attenuates renal ischemia/reperfusion injury. *Am J Pathol* 2001; **159**: 2137–2145.
36. Ramesh G, Reeves WB. TNF-alpha mediates chemokine and cytokine expression and renal injury in cisplatin nephrotoxicity. *J Clin Invest* 2002; **110**: 835–842.
37. Jaeschke H. Mechanisms of liver injury. II. Mechanisms of neutrophil-induced liver cell injury during hepatic ischemia-reperfusion and other acute inflammatory conditions. *Am J Physiol Gastrointest Liver Physiol* 2006; **290**: G1083–G1088.
38. Okusa MD. The inflammatory cascade in acute ischemic renal failure. *Nephron* 2002; **90**: 133–138.
39. Klausner JM, Paterson IS, Goldman G *et al.* Postischemic renal injury is mediated by neutrophils and leukotrienes. *Am J Physiol* 1989; **256**: F794–F802.
40. Benkoel L, Dodero F, Hardwigsen J *et al.* Effect of ischemia-reperfusion on bile canalicular F-actin microfilaments in hepatocytes of human liver allograft: image analysis by confocal laser scanning microscopy. *Dig Dis Sci* 2001; **46**: 1663–1667.
41. Kellerman PS, Norenberg SL, Jones GM. Early recovery of the actin cytoskeleton during renal ischemic injury *in vivo*. *Am J Kidney Dis* 1996; **27**: 709–714.
42. White SR, Williams P, Wojcik KR *et al.* Initiation of apoptosis by actin cytoskeletal derangement in human airway epithelial cells. *Am J Respir Cell Mol Biol* 2001; **24**: 282–294.
43. Haley M, Cui X, Minneci PC *et al.* Recombinant human activated protein C in sepsis: assessing its clinical use. *Am J Med Sci* 2004; **328**: 215–219.
44. Wang Y, Thiyagarajan M, Chow N *et al.* Differential neuroprotection and risk for bleeding from activated protein C with varying degrees of anticoagulant activity. *Stroke* 2008; **40**: 1864–1869.
45. Gale AJ, Sun X, Heeb MJ *et al.* Nonenzymatic anticoagulant activity of the mutant serine protease Ser360Ala-activated protein C mediated by factor Va. *Protein Sci* 1997; **6**: 132–140.
46. Gupta A, Gerlitz B, Richardson MA *et al.* Distinct functions of activated protein C differentially attenuate acute kidney injury. *J Am Soc Nephrol* 2009; **20**: 267–277.
47. SLOT C. Plasma creatinine determination. A new and specific Jaffe reaction method. *Scand J Clin Lab Invest* 1965; **17**: 381–387.
48. Kim J, Kim M, Song JH *et al.* Endogenous A1 adenosine receptors protect against hepatic ischemia reperfusion injury in mice. *Liver Transpl* 2008; **14**: 845–854.
49. Awad AS, Ye H, Huang L *et al.* Selective sphingosine 1-phosphate 1 receptor activation reduces ischemia-reperfusion injury in mouse kidney. *Am J Physiol Renal Physiol* 2006; **290**: F1516–F1524.
50. Herrmann M, Lorenz HM, Voll R *et al.* A rapid and simple method for the isolation of apoptotic DNA fragments. *Nucleic Acids Res* 1994; **22**: 5506–5507.
51. Molitoris BA. Putting the actin cytoskeleton into perspective: pathophysiology of ischemic alterations. *Am J Physiol* 1997; **272**: F430–F433.